Hindawi
International Journal of RF and Microwave Computer-Aided Engineering
Volume 2023, Article ID 6640730, 13 pages
https://doi.org/10.1155/2023/6640730

Research Article

Design and Characterization of a Compact Four-Element Microstrip Array Antenna for WiFi-5/6 Routers

Liton Chandra Paul,[1] **Sarker Saleh Ahmed Ankan**,[1] **Tithi Rani**,[2] **Md. Tanvir Rahman Jim**,[1] **Muharrem Karaaslan**,[3] **Sk. A. Shezan**,[4] **and Lulu Wang**[5]

[1]*Electrical, Electronic and Communication Engineering, Pabna University of Science and Technology, Bangladesh*
[2]*Electronics and Telecommunication Engineering, Rajshahi University of Engineering and Technology, Bangladesh*
[3]*Electrical and Electronics Engineering, Iskenderun Technical University, Hatay 31200, Turkey*
[4]*Electrical Engineering, Engineering Institute of Technology, Melbourne, Australia*
[5]*Biomedical Device Innovation Center, Shenzhen Technology University, Shenzhen 518118, China*

Correspondence should be addressed to Liton Chandra Paul; litonpaulete@gmail.com

Received 7 June 2023; Revised 25 June 2023; Accepted 5 August 2023; Published 17 August 2023

Academic Editor: Xiao Ding

The WiFi-5 band was the most popular WiFi band until the Federal Communications Commission (FCC) announced a new spectrum of 6 GHz WiFi (5.925–7.125 GHz) for unlicensed users. Our proposed work is about to cover both the 5 GHz and 6 GHz WiFi bands. These two bands have a great impact in the wireless communication field. A low-loss Rogers RT 5880 material is used as the substrate layer, which helps us to make the antenna compact ($23 \times 40 \times 0.79\,mm^3$) keeping a good performance profile over the latest high-speed WiFi-5/6 band. The proposed antenna covers a huge bandwidth (simulated BW: 2.85 GHz ranging from 4.50 to 7.35 GHz and measured BW: 2.83 GHz ranging from 4.50 to 7.33 GHz), which can be used for the latest WiFi-5 and WiFi-6 routers. The antenna also has omnidirectional properties. Besides that, the gain and directivity of the antenna are quite good, and the measured results buttress the simulated results. The presented different detail parametric studies indicate the antenna's optimization level, which is excellent. The minimum values of reflection coefficient and voltage standing wave ratio make it a compatible candidate for the implementation of high-speed WiFi-5/6 routers.

1. Introduction

Wireless fidelity (WiFi) depicts a fundamentally different approach to the airwaves that leads to a new era of wireless communications. WiFi refers to a wireless LAN technology that utilizes the IEEE 802.11 standards for wireless communications [1]. Using radio waves, it transmits data at high speed from a client device to an access point, such as a router, and the router completes a connection to other devices on the LAN, WAN, or Internet. The Internet is a wide area network (WAN) that transmits data using a series of protocols between networks and devices. Besides, WiFi simply connects devices without any cables. WiFi can also connect to the Internet via hotspots [2]. It is a secured process that can connect a huge number of clients [3, 4]. This is one of the top reasons for its wide use. WiFi hotspots are Internet access points that permit you to connect to a WiFi network through your smartphone, computer, or other devices. Various applications of WiFi enrich our communication sector, like mobile applications, home applications, business applications, automotive segments, video conferences, and browsing the Internet. WiFi technology does its job by using several frequency bands, such as 2.4 GHz, 5 GHz, and 6 GHz [5]. Among them, 6 GHz WiFi provides more speed for using a large number of channels [6–8]. It is the most recent WiFi technology. On April 23, 2020, the FCC agreed to adopt broad new provisions for wireless communication in the 6 GHz band, using 1200 MHz of spectrum for unlicensed devices [9, 10]. Unlicensed national information infrastructure (U-NII) radio bands, which make up the 6 GHz spectrum, include the following: U-NII-5 to U-

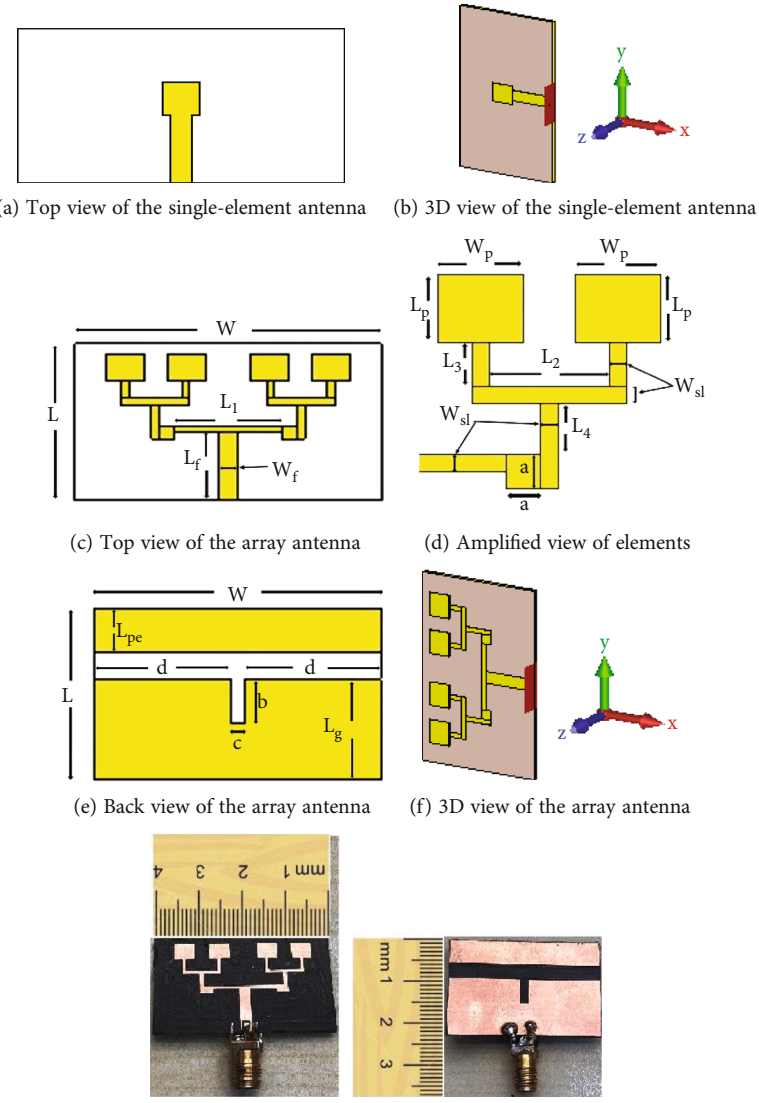

(a) Top view of the single-element antenna (b) 3D view of the single-element antenna

(c) Top view of the array antenna (d) Amplified view of elements

(e) Back view of the array antenna (f) 3D view of the array antenna

(g) Fabricated prototype of the array antenna

Figure 1: Proposed four-element antenna for WiFi-5/6 routers.

NII-8 [11, 12]. The band uses a frequency range of 5.925 GHz to 7.125 GHz [13]. The ongoing need for faster data rates has led to revolutionary advancements in the world of wireless gadgets. Modern multifunctional gadgets require a greater transmission data rate to ensure ultra-high-speed connectivity [14]. To prevent network data congestion caused by the excessive expansion of subscribers, big data rates and enormous capacity are required [15]. Aside from that, the 2.4 GHz band has a greater range of coverage but a slower data transfer speed, whereas the 5 GHz band has less coverage but a faster data transfer speed. The data transfer rate at higher frequencies is faster than at lower frequencies [16, 17]. Therefore, the 5 GHz band will transfer data at a higher speed than the 2.4 GHz band. The 6 GHz WiFi also provides lower latency and better battery life. The 5 GHz antenna has 23 channels for devices to use. It has a frequency range of 5.180 GHz to 5.925 GHz [18]. It occurs across a wide spectrum using numerous nonoverlapping channels with significant bandwidth. Orthogonal frequency division multiplexing (OFDM) makes 5 GHz resilient against interference that can occur from reflections [19]. Some WiFi routers and gadgets automatically use WiFi-5 channels. A router, which offers WiFi, is a device that is often connected to a modem. It transmits data from the Internet to portable electronics, including laptops, smartphones, and tablets. The maximum top speed of both 5 GHz and 6 GHz WiFi is 9.6 Gbps [20]. Sometimes, we suffer from buffering, but anyone can get over it by using the quickest WiFi-6 technology. The most recent generation of WiFi technology is WiFi-6 (802.11ax). For everyone to enjoy buffer-free streaming, faster downloads, and the expansion of additional smart home devices without compromising their online experience, it offers more trustworthy connections and faster WiFi speeds.

The work [21] introduces a dual-band WiFi antenna composed of a monopole and a capacitive coupled branch. It covers the 2.4 GHz and 5 GHz WiFi ranges. The bandwidths of this antenna are 112 MHz (2.374 GHz–2.486 GHz) and 1.026 GHz (4.678 GHz–5.704 GHz). The

Table 1: Geometrical parameters.

Description and symbol	Value (mm)
Substrate's length (L)	23
Substrate's width (W)	40
Substrate's thickness (h)	0.79
Metal's thickness (t)	0.035
Feeder's length (L_f)	10
Feeder's width (W_f)	2.50
Distance between T-junction microstrip power lines (L_1)	14
Distance between the feeders of patches in each group (L_2)	7
Length of feeder of each patch (L_3)	2.50
Length of strip line between two horizontally parallel strip lines (L_4)	3
Patch's length (L_p)	4
Patch's width (W_p)	5
Width of strip line (W_{sl})	1
a	2
b	6
c	2
d	19
Ground plane's length (L_g)	13.50
Parasitic element's length (L_{pe})	6

dimensions of the antenna are $80 \times 40 \times 0.5\,\text{mm}^3$ with 2 dB and 5 dB gain. The efficiency of the antenna for the lower band is above 70%, and for the higher band, the value is above 90%. A WiFi 2.4 GHz antenna is proposed in the work [22]. This metamaterial antenna's size is $40 \times 30 \times 1.6\,\text{mm}^3$. The antenna covers 0.574 GHz of bandwidth with 3.23 dB of gain, and the return loss of the antenna is quite low (-46.58 dB) at resonant frequency. A MIMO antenna for 5 GHz WiFi is presented in this paper [23]. The antenna also covers the band for WLAN and 5G applications. The bandwidth of the antenna is 4.58 GHz–6.12 GHz with a 4.02 dB gain. The antenna operates in the 5 GHz band, which is 5.35 GHz. This compact-sized ($30 \times 30 \times 0.8\,\text{mm}^3$) antenna has a good maximum efficiency of 96%. It varies from 67% to 82%. The authors in [24] proposed another dual-band antenna operating at 2.4 and 5 GHz. The antenna's bandwidth ranges from 2.24 GHz to 2.70 GHz when operating at 2.4 GHz and from 4.73 GHz to 5.6 GHz when operating at 5.0 GHz. The antenna provides a stable gain of 2.09 dB to 2.87 dB. The size of the antenna is about $50 \times 10 \times 1\,\text{mm}^3$. It is rare to find an antenna that covers 5 GHz and 6 GHz together. One of the reasons behind it is its latest addition to IEEE 802.11ax. In the early days, it was totally based on 2.4 GHz and 5 GHz. Now, 6 GHz WiFi is providing better facilities.

Our proposed work covers the latest WiFi-5/6 bands with higher efficiency and omnidirectional properties. Initially, we etched the design on the Rogers RT 5880 ($\varepsilon_r = 2.2$, $\tan\delta = 0.0009$) by using computer simulation technology in the microwave studio (CST MWS) and then fabricated it with the same material in the antenna laboratory. The dimension of our WiFi-5/6 antenna is $23 \times 40 \times 0.79$ mm^3. The paper is organized as follows: Section 2 discusses structural review with appropriate parameters. Section 3 talks all about simulated and fabricated results, including impactful and detailed parametric studies. And the conclusion is drawn in Section 4.

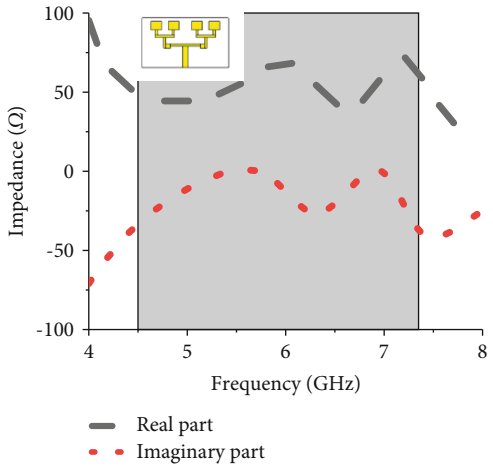

Figure 2: Z parameters (real and imaginary parts).

2. Wideband Antenna for WiFi-5/6 Routers

In order to do the initial modeling, we have used the high-performance 3D EM analysis software CST Microwave Studio (CST-MWS) for the four-element WiFi-5/6 antenna. Here, we have discussed all of the design strategies and geometrical issues of the proposed work. Figures 1(a)–1(g) show the top outlook of the single-element antenna, the 3D view of the single-element antenna, the top view of the array, the amplified view of the elements, the back view of the array, the 3D outlook of the array, and a fabricated prototype of the array with necessary labeling, respectively. An initial idea of the dimensions of the antenna has been estimated by the following equations: (1)–(4). Theoretically, the initial length and width of the rectangular patch are estimated at 0.21λ (17.26 mm) and 0.26λ (14.3 mm) with a full metallic ground plane, respectively. Then, the antenna is optimized to enhance performance by applying the sweep parameter method. A middle-slotted partial ground structure and a rectangular parasitic bar in the top of the ground plane have also been introduced during the optimization of the antenna. Finally, the optimized and reduced dimension of each patch element is achieved at $0.08\lambda\,(5\,\text{mm}) \times 0.06\lambda\,(4\,\text{mm})$ with a middle-slotted partial ground plane and a rectangular parasitic element. The proposed antenna is for the Rogers RT 5880, which has a dielectric constant of 2.2 and a loss tangent of 0.0009. The height of the substrate is 0.79 mm, and the area is $23 \times 40\,\text{mm}^2$ $(0.35\lambda \times 0.60\lambda)$. It is a four-element array antenna where four elements are divided into two groups.

$$\text{Patch width, } W_p = \frac{c}{2f_r}\sqrt{\frac{2}{\varepsilon_r + 1}}, \tag{1}$$

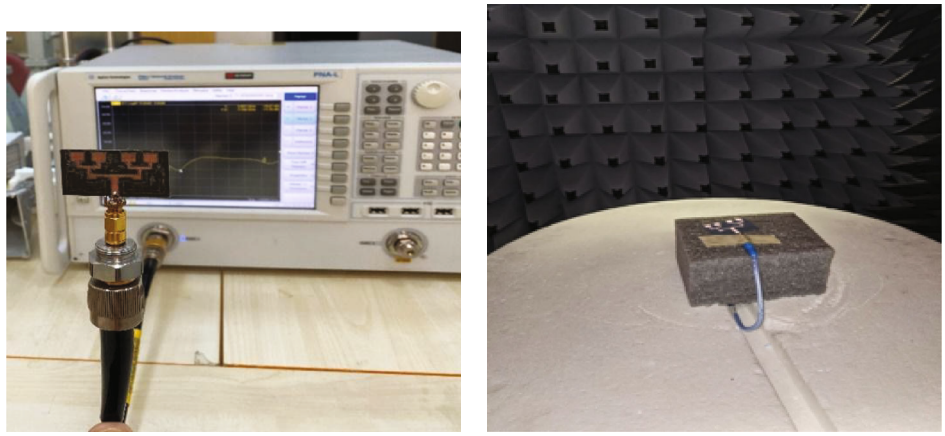

(a) Measurement setup with VNA (b) Measurement setup in anechoic chamber

FIGURE 3: Measurement setup in the antenna laboratory.

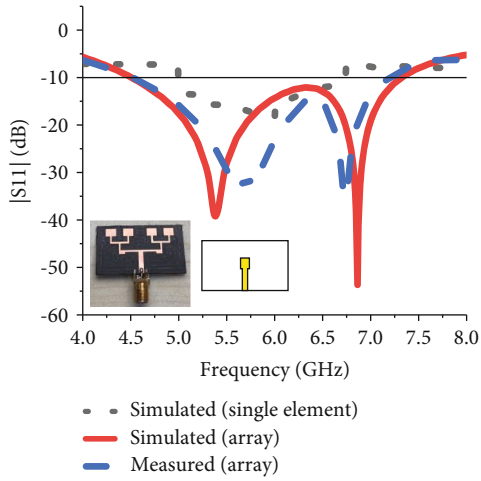

FIGURE 4: Reflection coefficient of the antenna.

where c is the velocity of light, f_r is the resonance frequency, and ε_r is the dielectric constant [25].

$$\text{Length, } L = 0.412h\frac{(\varepsilon_{reff} + 0.3)\left((W_p/h) + 0.264\right)}{(\varepsilon_{reff} - 0.258)\left((W_p/h) + 0.8\right)}, \quad (2)$$

$$\text{Effective length, } L_{eff} = \frac{c}{2f_r\sqrt{\varepsilon_{reff}}}, \quad (3)$$

$$\text{Patch length, } L_p = L_{eff} - 2\Delta L. \quad (4)$$

The designed feed network uses both the Wilkinson power divider and T-junction concepts. The size of the power divider determines the impedance matching [26]. The Wilkinson power divider approach enables isolation between output lines and matching of all individual input lines over the range of 50 Ω-70.7 Ω-100 Ω. By converting the 50 Ω feed line to 100 Ω lines using a quarter-wave transformer, an equal-split divider is created for 50 Ω input impedance systems. T-junction microstrip power dividers are used to power each patch element group from a 50 Ω input feeder. The size of the single patch element is $4 \times 5\,mm^2$. It is made of annealed copper material. The ground plane is also made of the same material, with a thickness of 0.035 mm. The patch elements are connected through different strip lines whose vivid measurements are shown in the amplified outlook, i.e., Figure 1(d). All the strip lines have the same width of 1 mm. On the back side of the four-element compact antenna, there is a slotted ground plane and a parasitic element. The length of the ground plane is 13.50 mm. A rectangular slot cuts the ground plane in the middle of it by $6 \times 2\,mm^2$. It enhances the bandwidth of the proposed antenna. The parasitic element covers the upper part of the ground plane with a length of 6 mm, which influences the gain of the antenna. All the optimized values of the geometrical parameters are listed in Table 1. The Z parameter of the compact WiFi-5/6 antenna is presented in Figure 2, which includes both real and imaginary parts of it. The quality factor of an antenna, which can provide information about the achievable bandwidth, is assessed using the Z parameter. Additionally, it can be helpful in creating an equivalent circuit model for the antenna [27]. The desired values for the real and imaginary parts of the Z parameter are 50 Ω and 0 Ω, respectively, at resonant frequencies. Our real part's values at the resonant frequencies of 5.382 GHz and 6.864 GHz are 50.426 Ω and 50.053 Ω, respectively. The imaginary values are -0.96284 Ω and 0.14337 Ω. Our two values, real and imaginary, are closed enough to the desired values.

3. Operating Principle, Results, and Discussion

The optimized patch elements as well as the use of four elements in the array lead to the ability to tune the array for the WiFi-5 and WiFi-6 router applications. For WiFi-5/6 routers, the array must be omnidirectional, which is made possible by the ground's slot and partial ground plane. The parasitic component is crucial in ensuring good gain and directivity across the WiFi-5/6 routers' working frequency range. In general, an array may generate a more effective, narrower electromagnetic beam than a single unit. To excite the target antenna, an AC power source is installed across the copper patch and the bottom ground layer of the dielectric Rogers RT 5880. The performance of the antenna as a whole is improved by the adoption of the low-loss Rogers

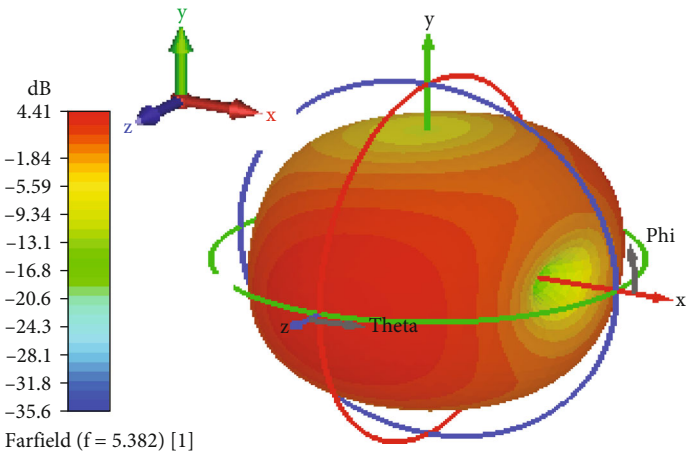

Farfield (f = 5.382) [1]

Type	Farfield
Approximation	Enabled …
Component	Abs
Output	Gain
Frequency	5.382 GHz
Rad. effic.	-0.1903 dB
Tot. effic.	-0.1909 dB
Gain	4.406 dB

(a) Gain (3D) at 5.382 GHz

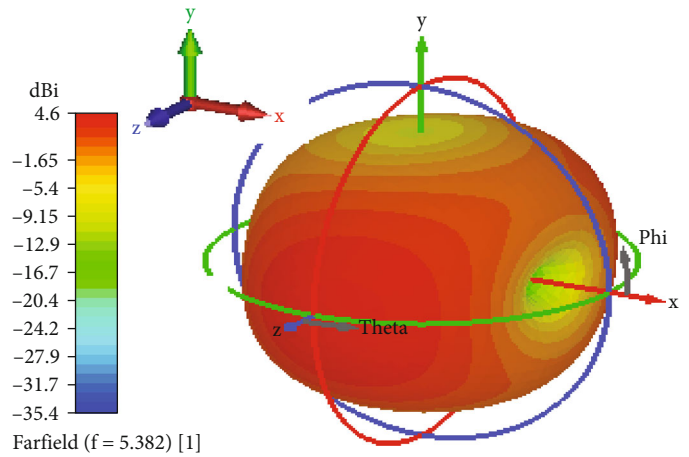

Farfield (f = 5.382) [1]

Type	Farfield
Approximation	Enabled …
Component	Abs
Output	Directivity
Frequency	5.382 GHz
Rad. effic.	-0.1903 dB
Tot. effic.	-0.1909 dB
Dir.	4.597 dBi

(b) Directivity (3D) at 5.382 GHz

Figure 5: Continued.

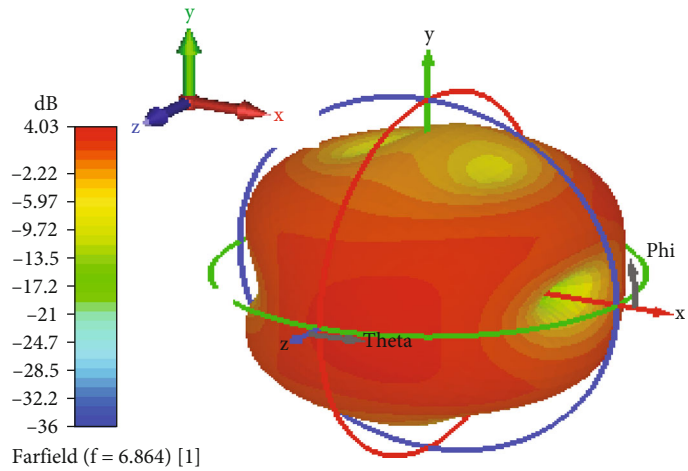

Farfield (f = 6.864) [1]

Type	Farfield
Approximation	Enabled …
Component	Abs
Output	Gain
Frequency	6.864 GHz
Rad. effic.	-0.2653 dB
Tot. effic.	-0.2653 dB
Gain	4.028 dB

(c) Gain (3D) at 6.864 GHz

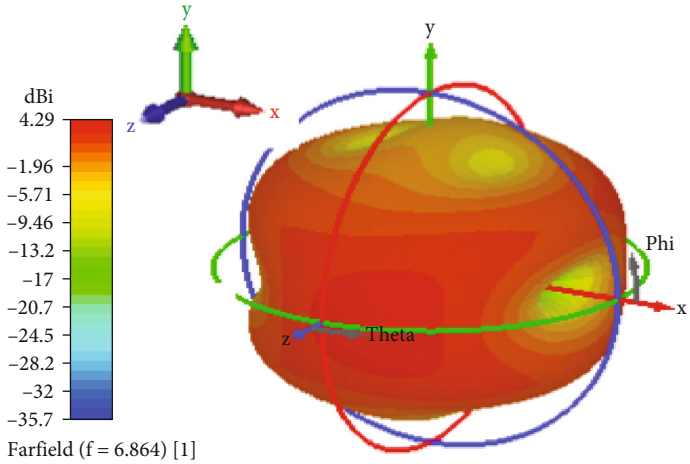

Farfield (f = 6.864) [1]

Type	Farfield
Approximation	Enabled …
Component	Abs
Output	Directivity
Frequency	6.864 GHz
Rad. effic.	−0.2653 dB
Tot. effic.	−0.2653 dB
Dir.	4.294 dBi

(d) Directivity (3D) at 6.864 GHz

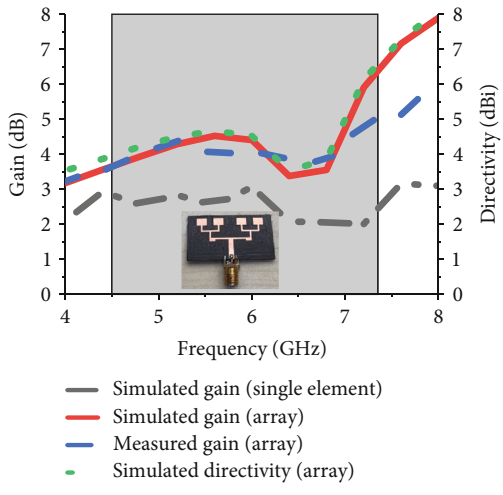

(e) Gain and directivity vs. frequency curve

Figure 5: Gain and directivity estimation of the designed antenna.

RT 5880. As current flowing through a feeder reaches the strip of the microstrip antenna, electromagnetic waves are created. The ensuing EM waves inside the substrate are reflected by the strip's margin due to the exceedingly thin strip line. The strip line is first divided into two arms, and then, those two arms are further divided into two branches. The splitting of strip lines and the impedance matching tasks were carried out using the Wilkinson power divider and T-junction principles. Electromagnetic waves are again released from each rectangle patch element when a sharp discontinuity happens. After fabrication, the prototype of the proposed four-element antenna is measured at an antenna measurement laboratory. A measurement setup with VNA has been presented in Figure 3(a), which is used to measure the reflection coefficient profile of the prototype. On the other hand, Figure 3(b) presents a photograph taken

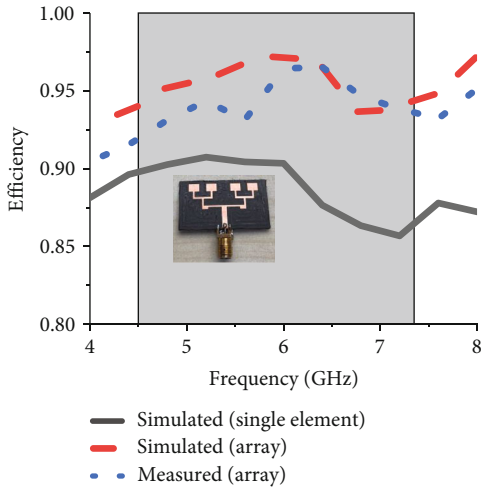

FIGURE 6: Radiation efficiency of the antenna.

within an anechoic chamber, which is used to measure the radiation properties like gain, efficiency, and radiation pattern of the prototype. In the anechoic chamber, an experimental setup consisting of the proposed array antenna prototype, an RF power transmitter, a receiver system, a positioning system, and a reference antenna with known gain is utilized to assess the prototype. By measuring the signal amplitude at the test antenna's receiver, the gain of the array antenna prototype is calculated. The gain of the fabricated array prototype is calculated using the Friis equation (5) from the measured reference antenna (transmitter) power (P_t), proposed fabricated array antenna (receiver) power (P_r), and reference antenna gain (G_r) [28]:

$$G\,(\mathrm{dBi}) = P_r\,(\mathrm{dBm}) - P_t\,(\mathrm{dBm}) - G_r\,(\mathrm{dBi}) + 20\log\left(\frac{4\pi R}{\lambda}\right)(\mathrm{dBi}), \tag{5}$$

where R is the distance between the reference antenna and test antenna. The efficiency of the antenna is determined by dividing the measurements from the transmitter and receiver of the test antenna prototype. The positioning system rotates the test antenna with respect to the reference antenna to figure out the radiation pattern as a function of angle.

The scattering parameter ($|S11|$ parameter) indicates the amount of reflection from the antenna. Greater reflection means greater loss, which is responsible for reducing efficiency. Therefore, keeping this $|S11|$ value as low as possible is good for an antenna system. Figure 4 depicts the initially designed and optimized rectangular single-element antenna's $|S11|$ parameter as well as our proposed wideband antenna's simulated and measured $|S11|$ parameter. The single-element antenna covers a bandwidth of 1.5 GHz ranging from 5 GHz to 6.5 GHz, with a reflection coefficient of -20 dB at 5.75 GHz. To enhance performance further, a 1×4 element array has been designed and optimized for WiFi-5/6 router applications. The simulated -10 dB impedance coverage band of the four-element array antenna is ranging from 4.50 GHz to 7.35 GHz, whereas the measured band is ranging from 4.50 GHz to 7.33 GHz. It resonates at two points: 5.382 GHz and 6.864 GHz. The simulated reflection coefficients at these points are -39.2 dB and -53.65 dB, respectively. The 2.85 GHz wide working band covers both the 5 GHz and 6 GHz WiFi bands, which is widely used for high-speed WiFi-5/6 routers, whereas the initially designed single-element antenna possesses lower performance for the intended router applications. WiFi-6 has enhanced security protocols for secure Internet use as well as backward compatibility with WiFi-5/2.4 devices. Although WiFi-5 gave us a gigabit connection, as more devices are added to the network, the smart home becomes smarter, and WiFi-5 falls short of providing the optimum WiFi experience. Orthogonal frequency division multiple access (OFDMA), a prime feature of WiFi-6, enables several devices with different bandwidth needs to connect to WiFi while also increasing overall network efficiency.

The maximum surface currents of the antenna are 70.2216 A/m at 5.382 GHz and 94.1871 A/m at 6.864 GHz. The density of current is higher from the T-junction power line to the lower part of the patch element as well as throughout the main feeder of the antenna. The gain and directivity characteristics of the suggested array antenna for WiFi-5/6 routers are summarized in Figure 5. The gain specifies the level of concentration of power supplied in a certain direction, whereas the directivity describes the amount of power transmitted in a specific direction. Directivity and efficiency are combined to form a gain. At the two distinct resonant frequencies of 5.382 GHz and 6.864 GHz, the 3D gain and 3D directivity are illustrated in Figures 5(a)–5(d), respectively. The array exhibits gains of 4.406 dB at 5.382 GHz and 4.028 dB at 6.864 GHz, respectively. For phi (ϕ) = 900, the curves of the Cartesian plot of gain at both frequencies of 5.382 GHz and 6.864 GHz can be presented for varying the value of theta (θ) from 0° to 180°. At both resonant points, the main lobe magnitudes of the Cartesian plots are 4.28 dB and 3.55 dB, respectively. The main lobes are directed at 180° with an angular width (3 dB) of 71.8° and 67.9° at 5.382 GHz and 6.864 GHz, respectively. The directivities are 4.597 dBi and 4.294 dBi, respectively, for the first and second resonant frequencies. The directivity and beamwidth are directly correlated with gain. Typically, the area covered decreases (measured in degrees) as the gain increases. Gain and beamwidth are perpetually oppositely correlated to one another. Last but not least, Figure 5(e) shows the simulated gain of the single-element antenna along with the simulated gain, measured gain, and simulated directivity of the proposed four-element antenna with respect to frequencies between 4 GHz and 8 GHz, where operating wideband is denoted by a gray-colored shadow. In comparison to a single-element antenna, the suggested four-element array antenna exhibits a much greater gain profile. The four-element antenna's gain and directivity profiles are consistent, and it has excellent omnidirectional performance. The antenna's practical use with WiFi-5/6 routers is made more credible by the fact that the measured gain closely tracks the simulated gain of the proposed array.

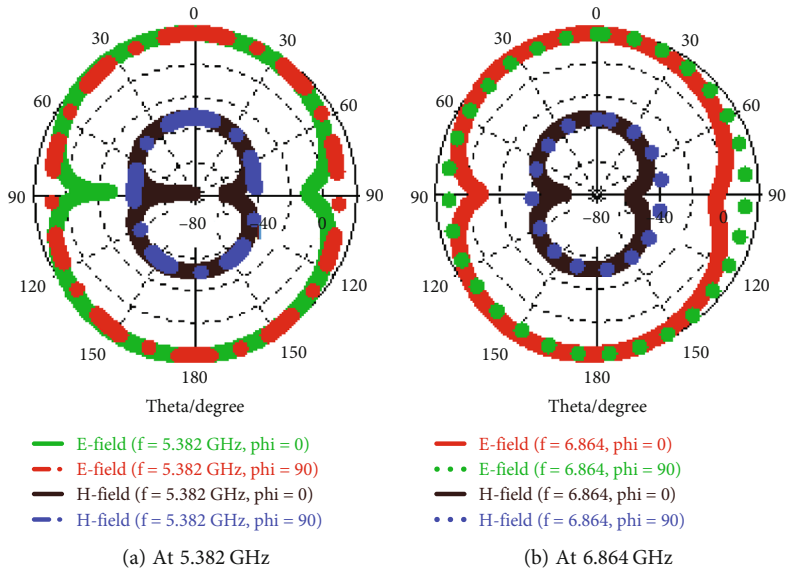

(a) At 5.382 GHz (b) At 6.864 GHz

FIGURE 7: *E*-field and *H*-field measurement.

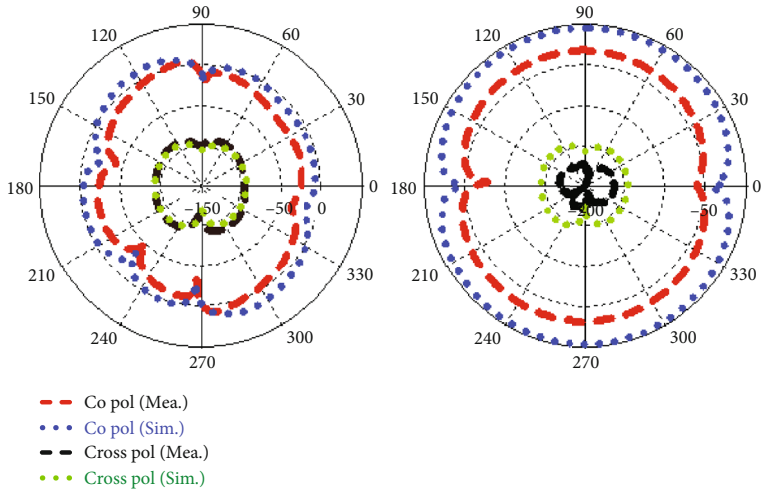

(a) For *E* plane (left) and *H* plane (right) at 5.382 GHz

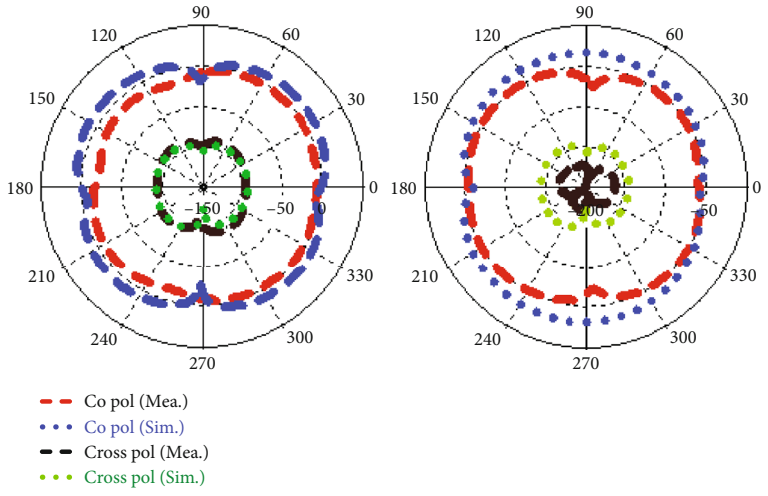

(b) For *E* plane (left) and *H* plane (right) at 6.864 GHz

FIGURE 8: Measured and simulated copolarization and cross-polarization.

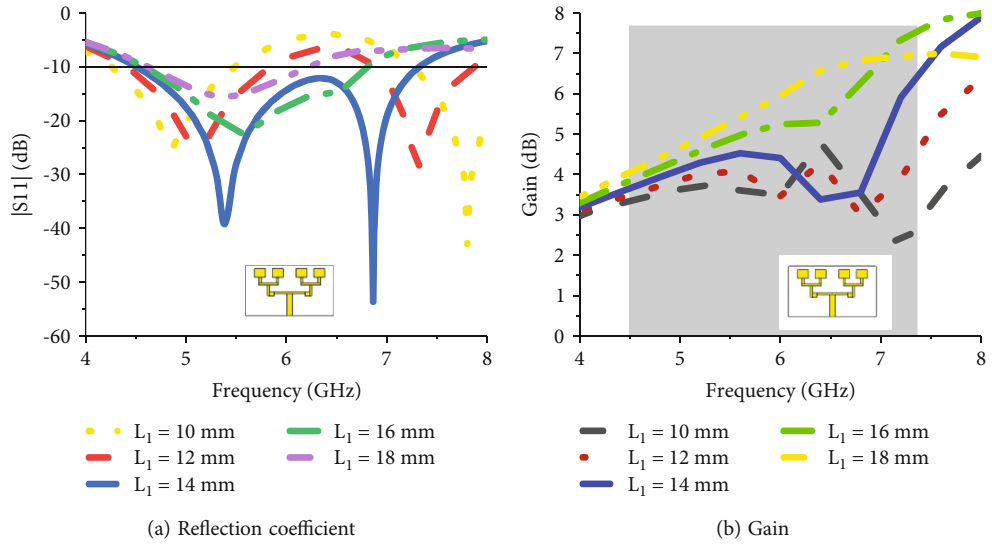

(a) Reflection coefficient (b) Gain

FIGURE 9: Impact of L_1 on reflection coefficient and gain.

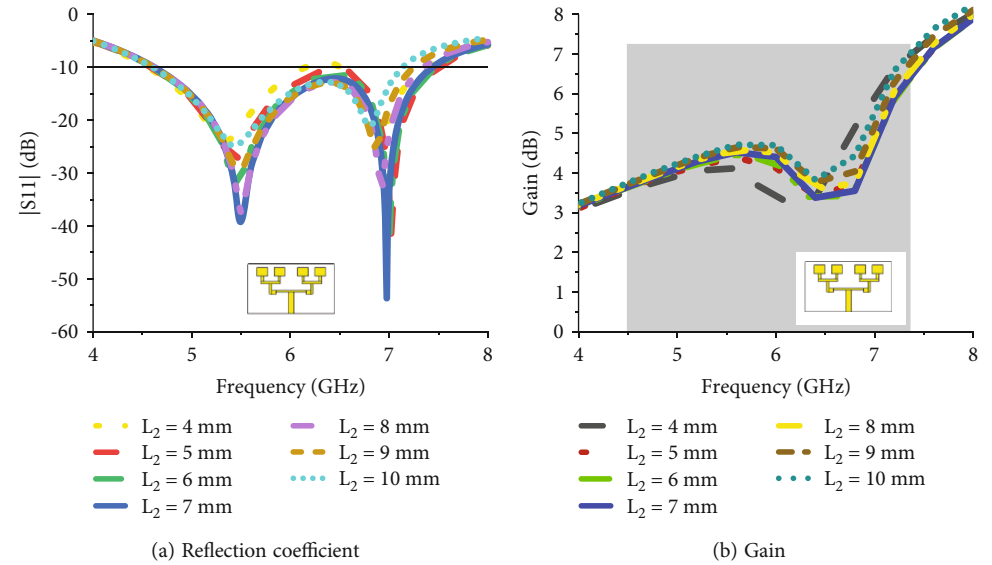

(a) Reflection coefficient (b) Gain

FIGURE 10: Impact of L_2 on reflection coefficient and gain.

The simulated efficiency of a single-element antenna and the measured and simulated radiation efficiency of the designed WiFi-5/6 array antenna are shown in Figure 6. It shows that the efficiency of the single-element antenna is lower than that of the array antenna. The simulated efficiency for a single element is about 85-91% whereas the efficiency of the WiFi array antenna is about 92–96.5% (measured) and 93.5–97.5% over its wide working frequency band, which is sufficiently high for high-speed WiFi-5/6 applications. The standing wave ratio calculates the amount of mismatch and assures maximum power transfer. The stable VSWR value is between 1 and 2. Here, the prototype shows lower values (1.0222 and 1.0042) at both resonant points and obeys the standard range within the wide working band for WiFi-5/6.

The radiation pattern of an antenna can be expressed by its electric field (E-field) pattern and its magnetic field (H-field) pattern. These values are taken for two values of phi (ϕ). One is for phi (ϕ) = 0°, and the other is for phi (ϕ) = 90°. The E-field pattern and H-field pattern at 5.382 GHz and 6.864 GHz are shown in Figures 7(a) and 7(b), respectively. From Figure 7(a), the main lobe magnitude of the E-field is 19.2 dBV/m at $\phi = 0°$ and 19.1 dBV/m at $\phi = 90°$. At $\phi = 0°$, the main lobe direction is 172° with an angular width (3 dB) of 80°. On the other hand, the main lobe direction is 180° with an angular width (3 dB) of 71.2° at $\phi = 90°$. Here, the main lobe magnitude of the H-field is -32.3 dBA/m at $\phi = 0°$ and -32.5 dBA/m at $\phi = 90°$. The direction and angular width (3 dB) of H-field are the same as those of E-field. The direction of the main lobe is 172° with an angular width (3 dB) of 80° at $\phi = 0°$, and the values are 180° and 71.2°, respectively, at $\phi = 90°$.

The E-field at $\phi = 0°$ has a magnitude of 18.8 dBV/m and is directed at 166°, as shown in Figure 7(b). Here, the angular

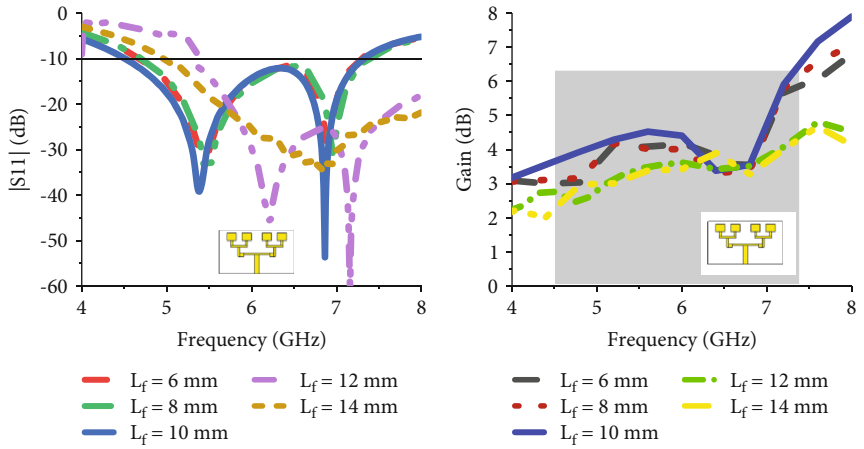

(a) Reflection coefficient (b) Gain

FIGURE 11: Impact of L_f on reflection coefficient and gain.

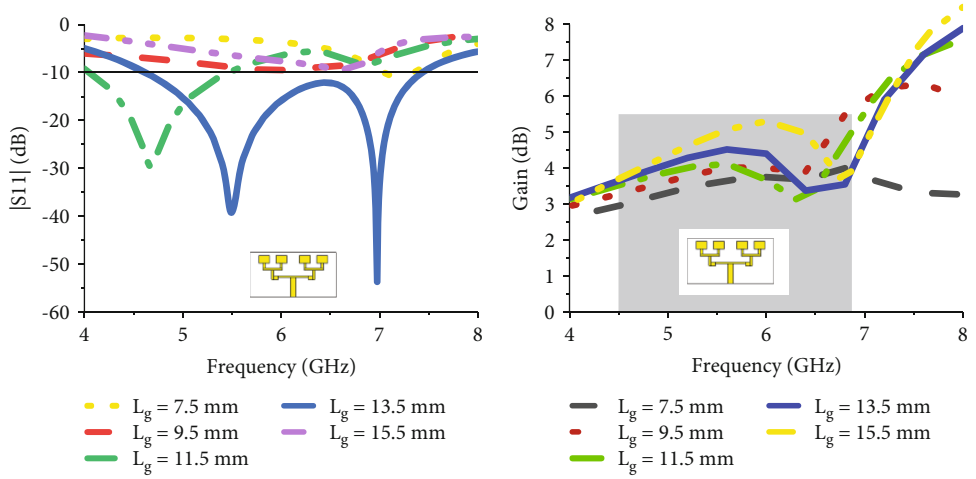

(a) Reflection coefficient (b) Gain

FIGURE 12: Impact of L_g on reflection coefficient and gain.

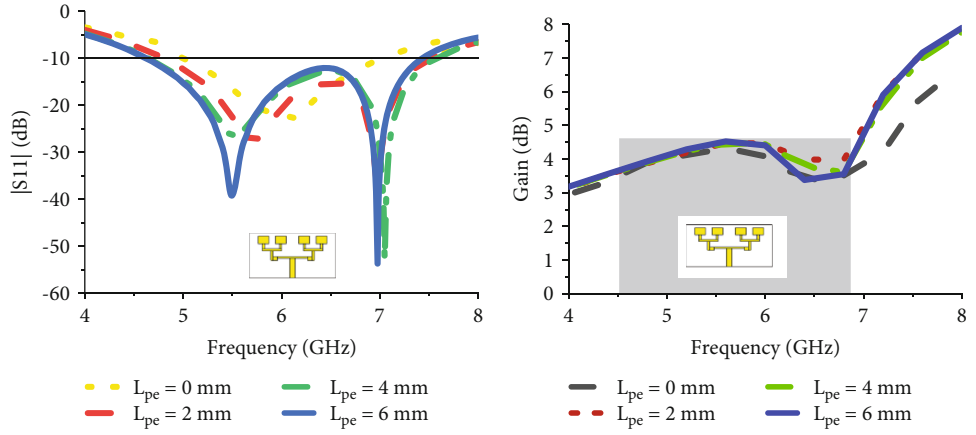

(a) Reflection coefficient (b) Gain

FIGURE 13: Impact of L_{pe} on reflection coefficient and gain.

Table 2: A comparison table with some relevant works.

Parameter	Reference works								This work
	[21]	[22]	[23]	[24]	[29]	[30]	[31]	[32]	
WiFi band (GHz)	2.4 and 5	2.4	5	2.4 and 5	6	5	5	5	5 and 6
Resonant frequency (GHz)	2.44, 5	2.4	5.35	2.4, 5	5.65	5.5	≈5	3.5, 5.2	5.382, 6.864
Return loss (dB)	≈ -30, ≈-30	-46.58	≈-26	≈-37, ≈-27	≈-35	-39.25	≈-42	≈-22, ≈-26	-39.2, -53.65
Bandwidth (GHz)	0.112, 1.026	0.574	1.54	0.46, 0.87	2	2.09	1.20	0.55,1.2	2.85
Maximum gain (dB)	2, 5	3.23	4.8	2.87	9	6.8	6	4.8	6.5
Maximum efficiency	90%	—	96%	—	—	—	81%	—	97.5%
Substrate material	FR4	FR4	FR4	FR4	PTFE	FR-4	FR-4	FR-4	Rogers RT 5880
Size ($L \times W \times h$) (mm^3)	$80 \times 40 \times 0.5$	$40 \times 30 \times 1.6$	$30 \times 30 \times 0.8$	$50 \times 10 \times 1$	$43 \times 39 \times 1.6$	$36 \times 36 \times 3.5$	$38 \times 36 \times 1.6$	$40 \times 29 \times 1.6$	$23 \times 40 \times 0.79$
Electrical size	$0.63\lambda \times 0.32\lambda$	$0.30\lambda \times 0.23\lambda$	$0.46\lambda \times 0.46\lambda$	$0.40\lambda \times 0.08\lambda$	$0.80\lambda \times 0.70\lambda$	$0.65\lambda \times 0.65\lambda$	$0.70\lambda \times 0.60\lambda$	$0.45\lambda \times 0.32\lambda$	$0.35\lambda \times 0.60\lambda$
Year	2020	2020	2020	2020	2019	2020	2020	2021	2023

width (3 dB) is 68.8° with a -1 dB side lobe level. It is 18.3 dBV/m with a direction of 180° at $\phi = 90°$ of the E-field main lobe magnitude. The angular width (3 dB) and side lobe level are the same as at $\phi = 0°$ which are 68.8° and -1 dB, respectively. For the H-field pattern at resonant frequency 6.864 GHz, the main lobe magnitude is -32.7 dBA/m and -33.2 dBA/m at $\phi = 0°$ and $\phi = 90°$, respectively. The main lobe's respective directions are 166° and 180°. At $\phi = 0°$, the angular width (3 dB) is 68.8° with a -1 dB side lobe level. At $\phi = 90°$, these values are 68.2° and -1 dB, respectively.

The simulated and measured copolarization and cross-polarization scenarios for both $E_{\phi=0}$ and $H_{\phi=0}$ planes of the fabricated prototype have been depicted in Figures 8(a) and 8(b) at both center operating frequencies of 5.382 GHz and 6.864 GHz, respectively. The antenna has a symmetrical radiation pattern at both frequencies of 5.382 GHz and 6.864 GHz.

In order to understand the radiation behavior of the designed WiFi-5/6 antenna, some geometrical parametric studies like the impact of the distance between T-junction microstrip power lines (L_1), the distance between the feeders of patches in each group (L_2), the length of the feeder (L_f), the length of the partial ground plane (L_g), and the length of the parasitic element (L_{pe}) have been performed in the 4–8 GHz frequency range.

With increasing the distance between two T-junctions of microstrip power line (L_1), the gain of the antenna increases, whereas the reflection profile shows most suitability at $L_1 = 14$ mm for the intended 5/6 GHz WiFi bands, and for the further increment of L_1, the antenna loses the suitability of the reflection profile for the WiFi-5/6 routers. Figures 9(a) and 9(b) show the effect of changing the distance between two T-junctions of the microstrip power line (L_1). As a result, the value of L_1 has a significant impact on both the reflection coefficient and the antenna gain.

The distance between the feeders of patches in each group (L_2) is changed from 4 mm to 10 mm, keeping the step size at 1 mm. As shown in Figure 10(a), the return loss decreases up to 7 mm before increasing. The gain of the antenna is comparatively less influenced by L_2 as presented in Figure 10(b); therefore, the optimized value of L_2 is set to 7 mm for the intended WiFi-5/6 router applications.

As shown in Figures 11(a) and 11(b), the length of the main feeder (L_f) has a significant impact on both the scattering parameter and the gain of the proposed WiFi-5/6 antenna. The designed prototype shows the most suitable scattering parameter and maximum gain for $L_f = 10$ mm. The range of gain is 3.4–6.5 dB over the targeted 5/6 GHz WiFi router applications.

To enhance both the reflection coefficient profile and the gain of the WiFi-5/6 antenna, a slotted partial ground plane and a parasitic element on the top part of the back side of the antenna have been introduced. The L_g can be adjusted in increments of 2 mm from 7.5 mm to 15.5 mm. The parameter L_g possesses a huge impact on the resonance of the prototype, as shown in Figures 12(a) and 12(b). Within the studied range of L_g, the antenna shows the best scattering matrix with suitable gain within the targeted coverage range of the high-speed WiFi-5/6 router. As per Figures 13(a) and 13(b), the length of the parasitic element also plays an important role in achieving optimized performance in the intended wideband applications. The optimized value of it is 6 mm.

To validate the nobility and strength of our work, a comparison between the proposed WiFi-5/6 router antenna and some recently published WiFi antennas is illustrated in Table 2. Our work ensures compactness ($23 \times 40 \times 0.79$ mm^3) with a maximum bandwidth of 2.85 GHz for the high-speed WiFi-5/6, the latest technology band for wireless routers.

4. Conclusion

This paper presents a four-element antenna for a wideband antenna operating at high speed on the latest WiFi-5/6 routers. The measurement results of the antenna prototype are well matched with simulated results, which ensures that it would be workable in both the 5 GHz and latest 6 GHz WiFi bands. The antenna uses a low-loss Rogers RT 5880 dielectric substrate, and copper (annealed) is used for the radiating patch and the ground plane. The proposed WiFi-5/6 antenna utilizes a T-junction microstrip power line to match impedance properly. This compact ($23 \times 40 \times 0.79$ mm^3) antenna provides omnidirectional properties with a huge bandwidth (simulated: 2.85 GHz and measured: 2.83 GHz) for the latest 5/6 GHz WiFi routers. It also possesses a good gain over the large operating band with higher efficiency (simulated: 93.5–97.5% and measured: 92–96.5%). The maximum directivity of the WiFi-5/6 antenna is 6.6 dBi. The port properties, like return loss and VSWR profiles, are very suitable for transferring maximum power from the input to the antenna. A detailed and impactful geometrical parametric study has also been presented and discussed in this paper. All these subsisting performances pledge that the antenna is apt for the latest high-speed WiFi-5/6 routers.

Data Availability

The data used to support the findings of this study are included within the article.

Conflicts of Interest

The authors declare that they have no conflicts of interest.

References

[1] D. L. Perez, A. G. Rodriguez, L. G. Giordano, M. Kasslin, and K. Doppler, "IEEE 802.11be extremely high throughput: the next generation of Wi-Fi technology beyond 802.11ax," *IEEE Communications Magazine*, vol. 57, no. 9, pp. 113–119, 2019.

[2] W. Xu, W. Shi, F. Lyu, H. Zhou, N. Cheng, and X. Shen, "Throughput analysis of vehicular Internet access via roadside WiFi hotspot," *IEEE Transactions on Vehicular Technology*, vol. 68, no. 4, pp. 3980–3991, 2019.

[3] N. Ivanov, J. Lou, and Q. Yan, "Smart WiFi: universal and secure smart contract-enabled WiFi hotspot," in *Security and Privacy in Communication Networks. SecureComm 2020. Lecture Notes of the Institute for Computer Sciences, Social*

Informatics and Telecommunications Engineering, pp. 425–445, Cham, 2020.

[4] S. Islam and M. N. Islam, "Design and implementation of login-based Wi-Fi hotspot network for an university campus," *Emerging Technologies in Data Mining and Information Security, Lecture Notes in Networks and Systems*, vol. 164, pp. 87–94, 2021.

[5] R. K. Saha, "Coexistence of cellular and IEEE 802.11 technologies in unlicensed spectrum bands -a survey," *IEEE Open Journal of the Communications Society*, vol. 2, pp. 1996–2028, 2021.

[6] S. Benkirane and M. Benaziz, "Performance evaluation of IEEE 802.11p and IEEE 802.16e for vehicular ad hoc networks using simulation tools," in *2018 IEEE 5th International Congress on Information Science and Technology (CiSt),*, pp. 573–577, Marrakech, Morocco, 2018.

[7] E. J. Oughton, W. Lehr, K. Katsaros, I. Selinis, D. Bubley, and J. Kusuma, "Revisiting wireless Internet connectivity: 5G vs Wi-Fi 6," *Telecommunications Policy*, vol. 45, no. 5, article 102127, pp. 1–15, 2021.

[8] G. Naik and J. M. J. Park, "Coexistence of Wi-Fi 6E and 5G NR-U: can we do better in the 6 GHz bands?," in *IEEE INFOCOM 2021 - IEEE Conference on Computer Communications*, pp. 1–10, Vancouver, BC, Canada, 2021.

[9] N. Yoza-Mitsuishi and P. Mathys, "Spectrum sharing between RLANs and terrestrial links in the 6 GHz band," in *2021 IEEE International Conference on Communications Workshops (ICC Workshops),*, pp. 1–7, Montreal, QC, Canada, 2021.

[10] M. A. Gregory, "5G and Wi-Fi 6 milestones," *Journal of Telecommunications and the Digital Economy*, vol. 8, no. 1, pp. 2–4, 2020.

[11] N. Y. Mitsuishi, P. Mathys, and D. Reed, "Spectrum sharing analysis for unlicensed use in 6 GHz using risk-informed interference assessment," in *47th Research Conference on Communication, Information and Internet Policy*, pp. 1–36, Elsevier, USA, 2019.

[12] E. Au, "6-GHz development in the United States [standards]," *IEEE Vehicular Technology Magazine*, vol. 14, no. 1, pp. 16–26, 2019.

[13] W. C. Jhang and J. S. Sun, "Small antenna design of triple band for WIFI 6E and WLAN applications in the narrow border laptop computer," *International Journal of Antennas and Propagation*, vol. 2021, Article ID 7334206, 8 pages, 2021.

[14] C. M. Krishna, S. Das, S. Lakrit, S. Lavadiya, B. T. P. Madhav, and V. Sorathiya, "Design and analysis of a super wideband (0.09–30.14 THz) graphene based log periodic dipole array antenna for terahertz applications," *Optik*, vol. 247, 2021.

[15] B. Aghoutane, S. Das, M. E. Ghzaoui, B. T. P. Madhav, and H. E. Faylali, "A novel dual band high gain 4-port millimeter wave MIMO antenna array for 28/37 GHz 5G applications," *AEU-International Journal of Electronics and Communications*, vol. 145, 2022.

[16] A. Z. Yonis, "Performance analysis of IEEE 802.11 ac based WLAN in wireless communication systems," *International Journal of Electrical and Computer Engineering*, vol. 9, no. 2, pp. 1131–1136, 2019.

[17] D. M. Greenwood, K. Y. Lim, C. Patsios, P. F. Lyons, Y. S. Lim, and P. C. Taylor, "Frequency response services designed for energy storage," *Applied Energy*, vol. 203, pp. 115–127, 2017.

[18] M. A. Haque, L. C. Paul, S. Kumar, R. Azim, M. S. Hosain, and M. A. Zakariya, "A plowing T-shaped patch antenna for WiFi and C band applications," *International Conference on Automation, Control and Mechatronics for Industry*, vol. 4, pp. 1–4, 2021.

[19] M. Debbah, B. Muquet, M. de Courville, M. Muck, S. Simoens, and P. Loubaton, "A MMSE successive interference cancellation scheme for a new adjustable hybrid spread OFDM system," *IEEE 51st Vehicular Technology Conference Proceedings*, vol. 2, pp. 745–749, 2000.

[20] M. Balkonis, *WIFI Evolution beyond WIFI 6, [M.S. thesis]*, Dept. of Digital Systems, University of Piraeus, 2021.

[21] Y. Ning, Y. Dong, Z. Wang, and Y. Fan, "A novel dual-band WIFI antenna with frequency-reconfigurability," in *2020 IEEE International Symposium on Antennas and Propagation and North American Radio Science Meeting*, pp. 67-68, Montreal, QC, Canada, 2020.

[22] G. Geetharamani and T. Aathmanesan, "Design of metamaterial antenna for 2.4 GHz WiFi applications," *Wireless Personal Communications*, vol. 113, no. 4, pp. 2289–2300, 2020.

[23] M. Yang and J. Zhou, "A compact pattern diversity MIMO antenna with enhanced bandwidth and high-isolation characteristics for WLAN/5G/WiFi applications," *Microwave and Optical Technology Letters*, vol. 62, no. 6, pp. 2353–2364, 2020.

[24] Y. B. Yang, F. S. Zhang, Y. Q. Zhang, and X. P. Li, "Design and analysis of a novel miniaturized dual-band omnidirectional antenna for WiFi applications," *Progress In Electromagnetics Research M*, vol. 94, pp. 95–103, 2020.

[25] L. C. Paul, H. K. Saha, T. Rani, M. Mahmud, T. K. Roy, and W. S. Lee, "An omni-directional wideband patch antenna with parasitic elements for sub-6 GHz band applications," *International Journal of Antennas and Propagation*, vol. 2022, Article ID 9645280, 8 pages, 2022.

[26] A. E. Alami, S. Das, B. T. P. Madhav, and S. D. Bennani, "Design, optimization and realization of high gain RFID array antenna 4×1 for detection system of objects in motion," *Journal of Instrumentation*, vol. 14, no. 5, pp. 1–14, 2019.

[27] L. C. Paul, H. K. Saha, T. Rani, R. Azim, M. T. Islam, and M. Samsuzzaman, "A dual-band semi-circular patch antenna for WiMAX and WiFi-5/6 applications," *International Journal of Communication Systems*, vol. 16, no. 1, article e5357, pp. 1–13, 2023.

[28] J. D. N. Cruz, A. J. R. Serres, A. C. D. Oliveira et al., "Bio-inspired printed monopole antenna applied to partial discharge detection," *Sensors*, vol. 19, no. 3, p. 628, 2019.

[29] K. Mondal and P. P. Sarkar, "Gain and bandwidth enhancement of microstrip patch antenna for WiMAX and WLAN applications," *IETE Journal of Research*, vol. 67, no. 5, pp. 726–734, 2021.

[30] J. Dong, C. Ding, and J. Mo, "A low-profile wideband linear-to-circular polarization conversion slot antenna using metasurface," *Materials*, vol. 13, no. 5, pp. 1–12, 2020.

[31] H. H. M. Ghouz, M. F. A. Sree, and M. A. Ibrahim, "Novel wideband microstrip monopole antenna designs for WiFi/LTE/WiMax devices," *IEEE Access*, vol. 8, pp. 9532–9539, 2020.

[32] P. R. Sura and M. Sekhar, "Circularly polarized dual band dual slot antenna for WLAN, Wi-MAX and Wi-Fi applications," *IETE Journal of Research*, vol. 69, no. 3, pp. 1550–1555, 2023.